Mechanism of efficient carbon monoxide oxidation at Ru (0001)

C. Stampfl and M. Scheffler

Fritz-Haber-Institut der Max-Planck-Gesellschaft, Faradayweg 4-6, D-14 195 Berlin-Dahlem,

Germany

(October 22, 2018)

We performed density-functional theory calculations using the generalized gradient approximation for the exhange-correlation functional to investigate the unusual catalytic behavior of Ru under elevated gas pressure conditions for the carbon monoxide oxidation reaction, which includes a particularly high CO_2 turnover. Our calculations indicate that a full monolayer of adsorbed oxygen actuates the high rate, enabling CO_2 formation via both scattering of gasphase CO molecules as well as by CO molecules adsorbed at oxygen vacancies in the adlayer, where the latter mechanism is expected to be very efficient due to the relatively weak adsorption energy of both CO and CO, as well as the close proximity of these reactants. In the present paper we analyse the bonding and electronic properties associated with the reaction pathway for CO_2 production via the scattering reaction. We find that the identified "bent" transition state is due to electron transfer into the unoccupied 2π orbitals of the CO molecule which reduces the Pauli repulsion between the impinging CO and the CO-covered surface. Bond formation to CO_2 then proceeds by electron transfer back from the CO 2π orbitals into the bonding region between CO and the adsorbed CO atom.

I. INTRODUCTION

Due to its fundamental importance and relative simplicity, the oxidation of carbon monoxide may be regarded as a prototype or model system of a heterogeneous catalytic reaction (molecular and dissociative (atomic) adsorption, surface reaction, desorption of products). This reaction has thus been extensively studied, and in many regards a good understanding has been established (see, for example Refs. [1–3] and references therein). To date, the reaction has always been found to proceed via the Langmuir-Hinshelwood (L-H) mechanism, i.e., reaction occurs between constituents that are both chemisorbed on, and in thermal equilibrium with, the surface. However, particularly interesting experimental results from recent elevated gas pressure catalytic reactor studies (e.g. operating at ~ 10 torr with CO/O₂ pressure ratios < 1) have been reported for the CO oxidation reaction over Ru (0001) [3,4] which led to the proposal that the Eley-Rideal (E-R) mechanism may be operational. In the E-R mechanism, the reaction takes place between particles in the qas-phase and particles chemisorbed on the surface. So far, E-R mechanisms, although discussed and speculated upon for the CO oxidation reaction in the past, have never been experimentally confirmed for this reaction. Firstly, these recent results found that the rate of CO₂ production is significantly higher than at other transition metal surfaces; in contrast, under ultra high vacuum (UHV) conditions, Ru (0001) is notably the poorest catalyst for this reaction [2]. Secondly, the measured kinetic data is markedly different to that of other substrates, and as opposed to other transition metal catalysts (Rh, Pt, Pd, and Ir), highest rates of CO_2 formation occur for high surface oxygen concentrations. Finally, almost no chemisorbed CO was detected during or after the reaction. The experimental findings described above for CO oxidation at Ru (0001) place a question mark over the reaction for this system; – in addition, one can also be placed over a microscopic understanding of this most basic heterogeneous catalytic reaction because to date it does not exist. This is largely because experiments are not readily able to probe the reaction from start to finish, i.e. they cannot follow the reaction pathway in microscopic detail; rather they offer information prior, and subsequent, to the reaction. In this respect theory can offer a way to obtain significant insight into how the reaction proceeds.

The majority of theoretical investigations of reactions at surfaces performed to date have used a cluster geometry, see e.g. Refs. [5,6] and references therein. In order to reduce (or avoid) possible problems with artificially localized wave functions and with cluster boundary conditions, we choose to use an extended surface by employing the supercell approach. The cell contains a number of atomic layers and a region of vacuum space. Thus the surface is extended in the x- and y-directions and is periodic on the scale of the supercell. The periodicity perpendicular to the surface should not play a role if the vacuum region is taken large enough. Such a supercell may thus be called a cluster where, however, in contrast to standard cluster calculations, the boundary conditions are treated chemically appropriately and the size of our "cluster" is significantly larger. In fact, due to the proper treatement of the boundary conditions, the results converge very fast and steadily with the cell size.

Numerous calculations have demonstrated that density functional theory (DFT) within the local density approximation (LDA) represents a good description of the quantum-mechanical many-body interactions for well-bonded situations. For less well-bonded situations, for example, transition-state geometries where bonds are in the process of being broken and reformed, e.g. dissociative adsorption and associative desorption, or for systems containing strong charge inhomogenuities, e.g. molecules at surfaces, recent results have revealed that the LDA can lead to inaccuracies. In this respect, using a generalized gradient approximation (GGA) for the exchange-correlation functional has been shown to significantly improve upon results obtained using the LDA (see for example, Refs. [7–10]). Some questions, however, have recently been raised concerning the accuracy of the GGA for the potential energy surfaces (PES's) for H₂ dissociation [11]. Nevertheless, the GGA is the best justified treatment for the exchange-correlation functional to date and we therefore choose to employ it in our present study. We like to note that due to recent theoretical developments and improved calculation methods as well as faster computers, it is only in the last couple of years that calculations of the type reported here have become possible for

reactions at surfaces; the studies performed to date have so far focused only on the "simple" dissociative adsorption of H_2 . The present study, the main results of which were reported earlier [12], represents the first investigation of a "real" surface chemical reaction (to be distinguished from dissociative chemisorption) using such theoretical methods.

In this paper we briefly describe the main results of our study and discuss the bonding and electronic structure of the identified reaction pathway for CO_2 formation via scattering of CO from the gas phase (g) and adsorbed (a) oxygen, i.e., $CO(g) + \frac{1}{2}O_2(a) \longrightarrow CO_2(g)$.

II. CALCULATION METHOD

We use density-functional theory (DFT) with the pseudopotential plane wave method and the supercell approach [13,14]. The surface is modelled using a (2×2) surface unit cell with four layers of Ru (0001) and a vacuum region equivalent to thirteen such layers. The ab initio fully separable pseudopotentials were created using the scheme of Troullier and Martins [15]. For the calculations discussed in the present paper, the plane wave cut-off was taken to be 40 Ry, with three **k**-points [16] in the surface Brillouin zone. The GGA of Perdew et al. [17] was employed for the exchange-correlation functional and it was used in creating the pseudopotential as well as in the total-energy functional. It is therefore treated in a consistent way, from the free atom to the solid surface and the reactants. The adsorbate structures were created on one side of the slab [13] where the position of all atoms were allowed to relax, except the bottom two Ru layers which were held at their bulk positions. For further details we refer to Refs. [12,18–20].

III. CO AT
$$(1 \times 1)$$
-O/RU (0001)

Earlier we reported results of DFT-GGA calculations for various adsorbate phases of oxygen on Ru (0001) [18] and found that a structure with a (1 × 1) periodicity and coverage $\Theta = 1$ should be stable on the surface where the oxygen atoms occupy the hcp hollow sites. (Here the coverage Θ is defined as the ratio of the concentration of adparticles to

that of substrate atoms in the topmost layer.) This result indicated that the formation of the $\Theta = 1$ structure under UHV conditions from gas phase O_2 is kinetically hindered, but that by using atomic oxygen (or high O_2 gas pressures), this phase should be attainable. Indeed this structure was successfully created under UHV by starting from the (2×1) phase with coverage $\Theta = 1/2$, obtained by exposing Ru (0001) to O₂ at room temperature, and then offering additional atomic oxygen to the surface via the dissociation of NO_2 [20]. The determined surface atomic structure of the (1×1) phase by the low-energy electron diffraction (LEED) intensity analysis of Ref. [20] agreed very well with that predicted by the DFT-GGA calculations. Furthermore, the calculations showed that the adsorption energy of oxygen in this phase is significantly weaker than in the lower coverage ordered phases of (2×1) and (2×2) periodicities; compare -1.89 eV to -2.33 eV and -2.60 eV, respectively, where the reference energy is taken to be that of $\frac{1}{2}O_2$. We note that evidence for higher oxygen coverages on Ru (0001) had been indicated by earlier experimental work; in particular, it had been proposed by Malik and Hrbek [21] that a three monolayer structure may form. Our more recent work [20], and that of Mitchell and Weinberg [22], however, showed that this structure is not realised. Instead, using NO₂, additional oxygen enters the bulk region after completion of the (1×1) O adlayer. Also, in the CO oxidation experiments performed at elevated gas pressures as described in the introduction, auger electron spectroscopy (AES) measurements indicated that there was one monolayer at the surface.

In our theoretical study, we therefore initially assumed that the (1×1) phase covered the surface and investigated the interaction of CO with this surface. To do this we calculated the energy for CO at various lateral positions and vertical positions over (1×1) -O/Ru (0001), i.e., we mapped the total energy on a three-dimensional grid over the surface. The results showed that CO cannot adsorb on the surface, – thus the L-H mechanism is completely inhibited by the presence of a perfectly ordered (1×1) O adlayer. The next step of our study was the consideration of an E-R mechanism as had been speculated upon on the basis of the experimental results. In order to do this, we evaluated an appropriate cut through the high-dimensional potential energy surface (PES); this cut is defined by the vertical position

of the C atom and the vertical position of the O adatom below the molecule. The resulting PES is presented in Fig. 1. In these calculations, the CO axis was held perpendicular to the surface (i.e., a "collinear" geometry) in order to ease the analysis. This restricted geometry was later released. At each point in the PES, the positions of all the atoms were relaxed except the bottom two Ru layers and the position of the C and O adatom which are fixed. From our results a reaction pathway for CO₂ formation via the E-R mechanism could be identified, where the associated activation energy barrier is about 1.6 eV. The PES in Fig. 1, indicates that CO_2 formation is achieved via an upward movement of the O adatom by ≈ 0.4 Å towards the incoming CO molecule when the molecule is in the range of 2.1 Å to 2.4 Å away from the surface. Because of the similar masses of C and O it is quite conceivable that a relatively energetic impinging CO molecule will impart a significant amount of energy to the O adatom, thus stimulating its vibrations and facilitating its motion (as indicated by the oscillations in the dot-dashed curve of Fig. 1). In this respect, we like to point out that the present system is notably different to H₂ dissociation in which the significant mass missmatch between the H atoms and atoms of the substrate makes it is reasonable to keep the substrate atoms rigid during the dissociation process. Due to the heavier reactant species of the present study, it is important to consider substrate relaxation. Such movement would then bring the system to the transition state of the reaction as denoted by the asterisk in Fig. 1. The calculation shows that the newly formed CO_2 molecule is strongly repelled from the surface and moves into the vacuum region with a significant energy gain of 1.95 eV.

On releasing the constraint that the CO axis be held perpendicular to the surface, we find that the activation energy barrier for CO_2 formation is reduced to 1.1 eV, and also that the position of the transition state for the reaction occurs closer to the surface (by 0.3 Å). The geometry of the transition state corresponds to one where the optimum tilt angle of the CO axis with respect to the surface normal is 49° which represents a "bond angle" of 131° for the " CO_2 -like" complex. It is interesting to note that this geometry is rather similar to that associated with the CO_2 —ion [23] and to that recently proposed for the "activated complex" (or transition state) for the CO oxidation reaction over other transition metal surfaces [24].

In order to understand the origin of the activation energy barrier for CO₂ formation, we analyse the layer-projected density of states (PDOS) and charge density and densitydifference distributions. At first it is instructive to consider the PDOS for the free CO and CO₂ molecules. Figure 2 shows the result for CO, where the upper and middle panels correspond to the projection of the wave function of the system onto the atomic orbitals of the O and C atoms, respectively. In the lower panel we show the PDOS for projection onto the O adatom. Similarly, Fig. 3 contains the result for free CO₂, where we show the result for just one O atom (the other is identical). The orbital energy levels of the molecules are indicated by standard notation appropriate to heteronuclear systems. We note that the energy zero for the PDOS of the free molecules have been aligned with that of the O/Ru (0001) surface. (This is useful for later discussion.) At this point it is informative to briefly describe the PDOS for the O adatom in the (1×1) O adlayer (lower panel of Fig. 2). A significant interaction of O 2p and Ru d states occurs, giving rise to bonding and antibonding states. These can be seen at energies of about -6.0 eV and 1.8 eV, respectively. In addition we note the existence of "non-bonding" O 2p states, largely of p_z -like character, in the energy region around -3 eV. We have found that the Ru d states involved in the bonding with the O 2p orbitals, the linear combination of which, result in an "effective" surface-related state that is located on the nearest-neighbor Ru atom and has two lobes, one of which is directed towards the O adatom (the spatial distribution is very similar to that visible in the right panels of Figs. 5 and 7). Furthermore, splitting of the O $2p_{x,y}$ states can be observed as the peaks in the region -6.0 to -7.0 eV; this is due to the O-O interaction as indicated by our calculations for a single (1×1) -O layer in vacuum. We refer to a forthcoming paper in which the bonding of O on Ru (0001) is described for the various ordered phases that form [25].

Considering now the PDOS for the collinear CO transition-state geometry, as shown in Fig. 4, from comparison with Fig. 2 the affect on the states of the impinging CO molecule and the O adatom can be observed due to their close proximity. Significant modifications can be noted: Firstly, some interaction of CO with the O adatom 2s orbital can be seen

for projection on the C atom as indicated by the small peak at about -19.0 eV. The CO 4σ level has moved to a lower energy (by 1.5 eV), as has the 1π level (by 1.3 eV). In this respect, the CO 4σ level appears to be interacting with the O $2p_z$ orbital of the O adatom as indicated by the small peak at about -10.0 eV. The CO 1π state similarly interacts with the O $2p_{x,y}$ states as suggested by the small peak at about -7.5 eV for projection on the O adatom. The most dramatic effect, however, is the strong interaction of the CO 5σ level (largely C-like) with the O $2p_z$ states which gives rise to new bonding and anti-bonding levels at about -8.0 eV and 3.0 eV, respectively. (It is to be noted that part of the CO 3σ -related state in Fig. 4 has been cut-off at high binding energy due to the too small energy window taken.) The various changes described in the PDOS are reflected in the density difference distributions. Figure 5 shows the total electron density and the density difference in the left and right panels, respectively. The density difference is obtained as the density of the complete system minus that of (1×1) -O/Ru (0001) and minus that of a free CO molecule. It can be noticed that there is charge depletion from the CO 5σ orbitals and from the O $2p_z$ orbitals of the adsorbed oxygen atom. An increase in electron density can be seen in the CO π orbitals and in the O $2p_{x,y}$ components. We can also see that charge has been transferred into d states of the nearest-neighbor Ru atom. These d states appear to be the same as those from which charge had been transferred in the formation of the (1×1) oxygen structure as briefly noted above. This movement of electron charge back towards the Ru atom weakens the O-Ru bond strength. These results suggest that the activation energy barrier is due to Pauli repulsion, predominantly between the O $2p_z$ states of the O adatom and the CO 5σ orbital which causes electron transfer into the CO π orbitals and into the O $2p_{x,y}$ states as well as back into neighboring Ru atoms. Furthermore, we note that the close presence of the closed-shell CO molecule to the (1×1) -O/Ru (0001) surface induces an average work function decrease of 0.35 eV. This is in marked contrast to the (1×1) O adlayer on Ru (0001), and to the other lower coverage ordered phases, for which the expected increase in work function occurs due to the high electronegativity of oxygen [26,27,18].

Understanding of the origin of the reduction in the activation barrier for CO₂ formation

(from 1.6 eV to 1.1 eV) on relaxing the constraint on the molecular axis and the reason for the tilt can be obtained by considering Figs. 6 and 7. These figures show the associated PDOS and electron density and density difference distributions, respectively, for the identified "bent" transition state. From Fig. 6 it can be seen that the most noticeable difference as compared to the results for the collinear transition state, is the development of states in the region of the Fermi level (both above and below). These states can be seen most clearly for projection on the C and O $2p_x$ orbitals. We will come back to this point later. Futhermore, splitting of the PDOS of the C and O $2p_{x,y}$ states due to the reduced symmetry can be observed. Similarly to the results of the PDOS for the collinear transition state, the CO 4σ interacts with the O $2p_z$ state; here however, the interaction is considerably stronger. Again the CO 5σ interacts with the highest lying O $2p_z$ state giving rise to bonding and anti-bonding states. On investigating the spatial distribution of these states in the region of the Fermi level, we find that they involve the mentioned Ru d states, states of the O adatom, and the 2π orbitals of CO, where for the latter, only the "upper" (furthest away from the surface) lobe is involved. Partial electron occupation of this previously unoccupied state gives rise to the "tilted" or "bent" atomic configuration of the transition state. Further understanding of these bonding rearrangements can be obtained from the density difference distributions as given in Fig. 7. The redistribution of electron charge is similar to that of Fig. 5, with the notable difference however that there is a significantly larger increase of electron density into the π orbitals of the CO molecule; for the C atom this is for mainly just one of the lobes. This region of charge increase corresponds to that of the states described above in the PDOS of Fig. 6 which form around the Fermi level, i.e. those involving the CO 2π orbitals.

From the above analysis, it thus appears that the microscopic picture of CO_2 formation via the scattering of CO is as follows: There is an initial repulsive interaction of CO with the O-covered surface due to Pauli repulsion between the closed-shell CO and the partially negatively charged O adatom, in particular, between the CO 5σ and the O $2p_z$ states. This interaction serves to reduce the O-Ru bond strength. The repulsive interaction is noticeably

reduced by a "bent" configuration since in this geometry charge transfer may occur into the unoccupied 2π orbitals, thus reducing the repulsion. Bond formation between CO and O to produce CO₂ then proceeds by charge transfer back from the 2π orbital into the region of the new bond. It is conceivable that this process, i.e., the role of the CO 2π orbitals and the weakening of the adsorbate-substrate bonds by charge transfer back towards the substrate due to the repulsive interaction, may be quite general and we speculate that it could in fact be the microscopic process by which oxidation of CO by adsorbed O usually proceeds also in the case of the L-H mechanism on transition metal surfaces.

We now ask whether the scattering reaction mechanism for CO₂ production, described above can explain the unusually high rate reported. From a rough estimate of the rate [28] we find that it is significantly lower than that observed in the elevated pressure experiments. This indicates that this mechanism alone is not responsible for the high turn-over frequency of CO₂. Nevertheless, were molecular beam experiments to be performed, CO₂ formation via this E-R process may be identified. To understand the reported high rate we turn to another consideration: Once a CO₂ molecule has formed and has left the surface (e.g. by the above described E-R reaction) there will be an oxygen vacancy in the adlayer. This site will be occupied by either CO or $\frac{1}{2}$ O₂ from the gas phase. Our calculations for the adsorption of the O_2 dimer at such a vacancy showed that it is unstable. On the other hand, we find that CO can weakly adsorb in an O vacancy with an adsorption energy is 0.85 eV. This value is significantly less than that which we calculate for CO on the clean surface, and on the surface with adsorbed oxygen, for oxygen coverages less than half a monolayer [19]. [On the clean surface, using the same (2×2) periodicity as the rest of the calculations (rather than the $(\sqrt{3} \times \sqrt{3})R30^{\circ}$ structure that actually forms), the value obtained is 1.68 eV; the experimental value has been reported to be 1.66 eV [29].] Adsorption of $\frac{1}{2}O_2$ (i.e., an O atom from O_2) in such a vacancy is more favorable, where the adsorption energy is 1.20 eV. Assuming thermal equilibrium and using the law of mass action [30] the calculated energies imply that 0.03 % of sites in the O adlayer will be occupied by CO. Chemisorption of $\frac{1}{2}O_2$ in the vacancy, however, from O_2 gas will be hindered by an energy barrier for dissociation [20,22] whereas CO may occupy this site essentially without hindrance. This means that the actual concentration of adsorbed CO will be somewhat higher than that estimated above. Reaction to CO₂ from CO at the vacancy and a neighboring O adatom (the surface reaction step of the heterogeneous cycle), is calculated to give rise to an energy gain of ≈ 0.66 eV. This value is obtained as the difference between the reaction energy in vacuum and the sum of the adsorption energies of O and CO on the surface prior to reaction. This value is noticeably smaller than that of 1.95 eV as we obtained for the E-R mechanism, but is still quite large if compared to that of $\approx 0.2 \text{ eV}$ as obtained experimentally for CO oxidation over Pt (111) and Pd (111) [2]. We do note that some of this energy may be disipated to phonons, thus reducing the value somewhat. A L-H reaction between the adsorbed CO molecule in a vacancy and a neighboring O adatom is expected to be particularly efficient and to give rise to the high rate due to the mentioned weaker bond strengths of both the adsorbed CO molecule and the O adatom, as well as their close proximity to one another. As noted in the introduction, under UHV conditions, ruthenium is the least efficient catalyst for the CO oxidation reaction. This is likely to be related to the fact that for low oxygen coverages ($\Theta \leq 0.5$) as occurs under UHV, ruthenium binds oxygen (and carbon monoxide) particularly strongly. From simple arguments, this is likely to lead to a lower reaction rate as compared to that over other transition metal catalyts, which under the same condictions, bind these particles less strongly.

REFERENCES

- [1] T. Engel and G. Ertl, Adv. Catal. 28, 1 (1979).
- [2] The chemical physics of solid surfaces and heterogeneous catalysis, eds. D. A. King and
 D. P. Woodruff, Vol. 4, Elsevier (1982) and references therein.
- [3] C. H. F. Peden, in Surface Science of Catalysis: In situ probes and reaction kinetics, eds. D. J. Dwyer and F. M. Hoffmann, Am. Chem. Soc., Washington DC (1992).
- [4] C. H. F. Peden, D. W. Goodman, M. D. Weisel, and F. Hoffmann, Surf. Sci. 253, 44 (1991).
- [5] E. J. Baerends, Prog. in Phys., to be published.
- [6] J. L. Whitten and H. Yang, Surf. Sci. Rep. 24, 55 (1996).
- [7] P. H. T. Philipsen, G. te Velde, and E. J. Baerands, Chem. Phys. Lett, 226, 583 (1994).
- [8] P. Hu, D. A. King, S. Crampin, M.-H. Lee, and M. C. Payne, Chem. Phys. Lett. 230, 501 (1994).
- 9 B. Hammer, K. W. Jacobson, and J. K. Nørskov, Phys. Rev. Lett. **70**, 3971 (1993).
- [10] M. R. Pederson, to be published.
- [11] P. Nachtigall, K. D. Jordan, A. Smith, and H. Jónsson, to be published.
- [12] C. Stampfl and M. Scheffler, to be published.
- [13] J. Neugebauer and M. Scheffler, Phys. Rev. B 46, 16067 (1992).
- [14] R. Stumpf and M. Scheffler, Comp. Phys. Commun. **79**, 447 (1994).
- [15] N. Troullier and J. L. Martins, Phys. Rev. B 43, 1993 (1991).
- [16] S. L. Cunningham, Phys. Rev. B 10, 4988 (1974).
- [17] J. P. Perdew, J. A. Chevary, S. H. Vosko, K. A. Jackson, M. R. Pederson, D. J. Singh,

- and C. Fiolhais, Phys. Rev. B 46, 6671 (1992).
- [18] C. Stampfl and M. Scheffler, Phys. Rev. B, **54**, 2868 (1996).
- [19] C. Stampfl, Surf. Rev. Lett., in press.
- [20] C. Stampfl, S. Schwegmann, H. Over, M. Scheffler, and G. Ertl, Phys. Rev. Lett., 77, 3371 (1996).
- [21] I. J. Malik and J. Hrbek, J. Vac. Sci. Technol. A 10, 2565 (1992).
- [22] W. J. Mitchell and W. H. Weinberg, J. Chem. Phys. 104, 9127 (1996).
- [23] J. Pacansky, U. Wahlgren, and P. S. Bagus, J. Chem. Phys. **62** (1975) 2740.
- [24] G. W. Coulston and G. L. Haller, J. Chem. Phys. 95 (1991) 6932, and references therein.
- [25] C. Stampfl and M. Scheffler, to be published.
- [26] T. E. Madey, H. A. Engelhardt, and D. Menzel, Surf. Sci. 48, 304 (1975).
- [27] L. Surnev, G. Rangelov, and G. Bliznakov, Surf. Sci. **159**, 299 (1985).
- [28] For our estimate we use the frequency of impinging CO molecules per surface Ru atom of $\nu = 7.5 \times 10^6 \, s^{-1}$ as the prefactor which corresponds to a CO gas phase pressure of 16 torr, and the temperature is taken to be $T = 500 \, \text{K}$.
- [29] H. Pfnür, P. Feulner, H. A. Engelhardt, and D. Menzel, Chem. Phys. Lett. 59, 481 (1978).
- [30] We assumed that the O_2 and CO partial pressures are equal, the temperature is T = 500 K, and the binding energy of CO into an O-vacancy in the (1×1) O adlayer is calculated to be by 0.35 eV less favorable than that of $\frac{1}{2}$ O_2 .

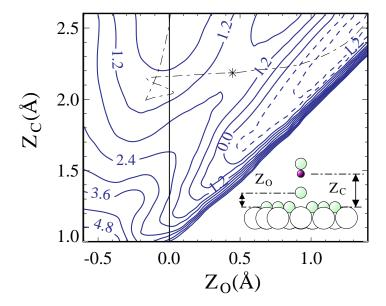


FIG. 1. Potential energy surface (PES) as a function of the positions of the C atom, $Z_{\rm C}$, and of the O adatom, $Z_{\rm O}$. Positive energies (i.e. repulsion) are shown as continuous lines, negative ones (i.e. energy gain) as dashed lines. The contour-line spacing is 0.6 eV.

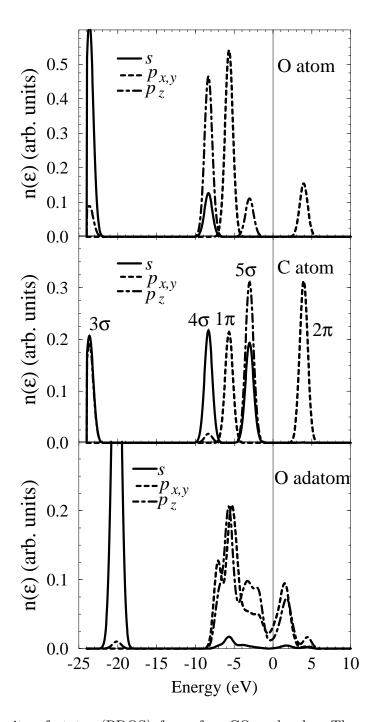


FIG. 2. Projected density of states (PDOS) for a free CO molecule. The upper, middle, and lower panels correspond to projection on the O and C atoms of CO, and on the O adatom, respectively.

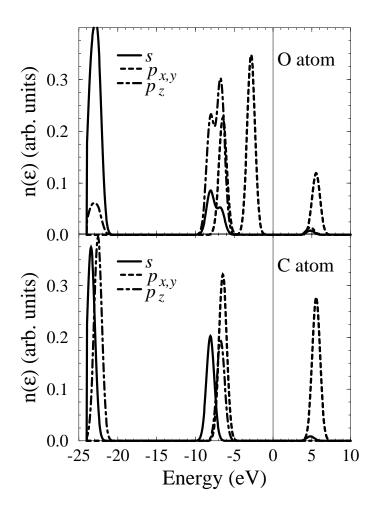


FIG. 3. Projected density of states (PDOS) for a free CO₂ molecule. The upper and lower panels correspond to projection on the O and C atoms, respectively.

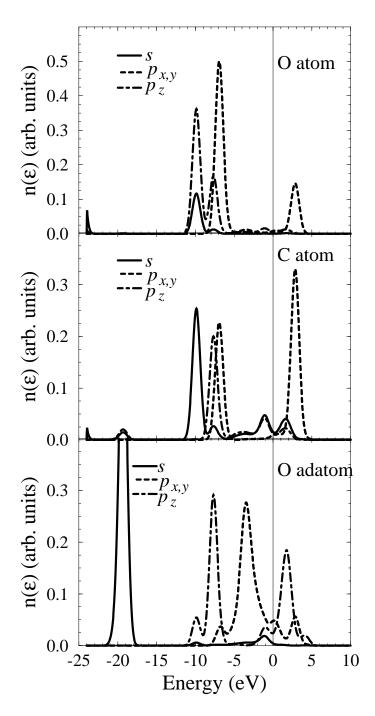


FIG. 4. Projected density of states (PDOS) for the "collinear" transition state for reaction via scattering of CO from (1×1) -O/Ru (0001). The upper, middle, and lower panels correspond to projection on the O and C atoms of CO, and on the O adatom, respectively.

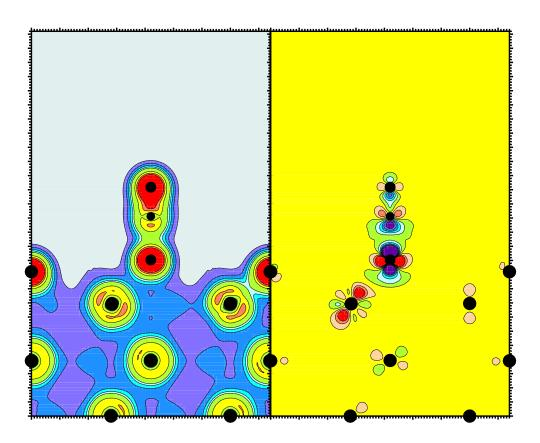


FIG. 5. Electron density (right panel) and density difference (left panel) distributions for the "collinear" transition state. The contours for the electron density are such that the spacing of the first five contour lines is 2.0, where the first line begins at 2.0. Thereafter the spacing is 10.0. For the density difference, the contour spacing is 0.6 where the first positive countour line begins at 0.3 and the first negative one at -0.3. The warm (orange, red) and cool (green, blue, purple) colors represent regions of charge increase and decrease, respectively. The units are $10^{-2}e/a_0^3$.

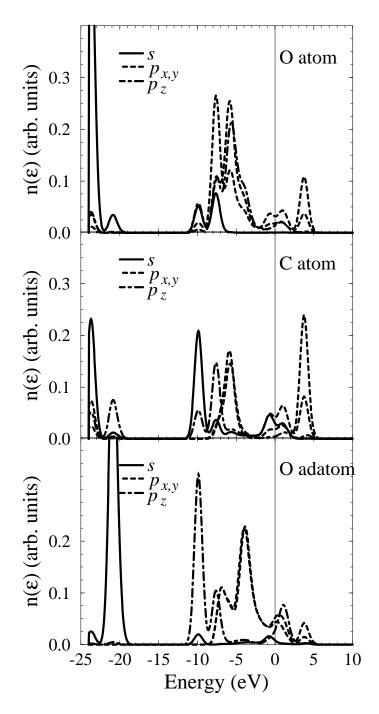


FIG. 6. Projected density of states (PDOS) for the identified "bent" transition state for reaction via scattering of CO from (1×1) -O/Ru (0001). The upper, middle, and lower panels correspond to projection on the O and C atoms of CO, and on the O adatom, respectively.



This figure "fig7.gif" is available in "gif" format from:

http://arxiv.org/ps/cond-mat/9611220v1